



Universiteit
Leiden
The Netherlands

Parasitic small-moment antiferromagnetism and nonlinear coupling of hidden order and antiferromagnetism in URu₂Si₂ observed by Larmor diffraction

Niklowitz, P.G.; Pfeiderer, C.; Keller, T.; Vojta, M.; Huang, Y.K.; Mydosh, J.A.

Citation

Niklowitz, P. G., Pfeiderer, C., Keller, T., Vojta, M., Huang, Y. K., & Mydosh, J. A. (2010). Parasitic small-moment antiferromagnetism and nonlinear coupling of hidden order and antiferromagnetism in URu₂Si₂ observed by Larmor diffraction. *Physical Review Letters*, 104(10), 106406. doi:10.1103/PhysRevLett.104.106406

Version: Not Applicable (or Unknown)

License: [Leiden University Non-exclusive license](#)

Downloaded from: <https://hdl.handle.net/1887/61339>

Note: To cite this publication please use the final published version (if applicable).

Parasitic Small-Moment Antiferromagnetism and Nonlinear Coupling of Hidden Order and Antiferromagnetism in URu_2Si_2 Observed by Larmor Diffraction

P. G. Niklowitz,^{1,2} C. Pfleiderer,¹ T. Keller,^{3,4} M. Vojta,⁵ Y.-K. Huang,⁶ and J. A. Mydosh⁷

¹Physik Department E21, Technische Universität München, 85748 Garching, Germany

²Department of Physics, Royal Holloway, University of London, Egham TW20 0EX, United Kingdom

³ZWE FRM II, Technische Universität München, 85748 Garching, Germany

⁴Max-Planck-Institut für Festkörperforschung, Heisenbergstrasse 1, 70569 Stuttgart, Germany

⁵Institute for Theoretical Physics Universität zu Köln, Zülpicher Strasse 77, 50937 Köln, Germany

⁶Van der Waals-Zeeman Institute, University of Amsterdam, 1018XE Amsterdam, The Netherlands

⁷Kamerlingh Onnes Laboratory, Leiden University, 2300RA Leiden, The Netherlands

(Received 10 September 2009; published 12 March 2010)

We report for the first time simultaneous microscopic measurements of the lattice constants, the distribution of the lattice constants, and the antiferromagnetic moment in high-purity URu_2Si_2 , combining Larmor and conventional neutron diffraction at low temperatures and pressures up to 18 kbar. Our data demonstrate quantitatively that the small moment in the hidden order (HO) of URu_2Si_2 is purely parasitic. The excellent experimental conditions we achieve allow us to resolve that the transition line between HO and large-moment antiferromagnetism (LMAF), which stabilizes under pressure, is intrinsically first order and ends in a bicritical point. Therefore, the HO and LMAF must have different symmetry, which supports exotic scenarios of the HO such as orbital currents, helicity order, or multipolar order.

DOI: 10.1103/PhysRevLett.104.106406

PACS numbers: 71.27.+a, 61.05.F-, 62.50.-p, 75.30.Kz

For over 20 years one of the most prominent unexplained properties of f -electron materials has been a phase transition in URu_2Si_2 at $T_0 \approx 17.5$ K into a state known as “hidden order” (HO) [1–3]. The discovery of the HO was soon followed by the observation of a small antiferromagnetic moment (SMAF), $m_s \approx 0.01\text{--}0.04\mu_B$ per U atom [4] then believed to be an intrinsic property of the HO. The discovery of large-moment antiferromagnetism (LMAF) of $m_s \approx 0.4\mu_B$ per U atom [5] under pressure consequently prompted intense theoretical efforts to connect the LMAF with the SMAF and the HO. In particular, models have been proposed that are based on competing order parameters of the *same* symmetry and hence linearly coupled in a Landau theory; such models assume that the SMAF is intrinsic to the HO [6–9]. This is contrasted by proposals for the HO parameter such as incommensurate orbital currents [10], multipolar order [11], or helicity order [12], where HO and LMAF break *different* symmetries.

The relationship of the symmetry of HO and LMAF, which clearly yields the key to the HO [8,9], has not been resolved. While some neutron scattering studies of the temperature-pressure phase diagram suggest that the HO–LMAF phase boundary ends in a critical end point [13,14], other studies concluded that it meets the boundaries of HO and LMAF in a bicritical point [15–18]. This distinction is crucial, as a critical end point (bicritical point) implies that HO and LMAF have the same (different) symmetries, respectively [9]. Moreover, there is a substantial disagreement with respect to the location and shape of the HO–LMAF phase boundary (see, e.g., Refs. [14,19]). This lack of consistency is, finally, accompanied by considerable variations of the size and pressure

dependence of the moment reported for the SMAF [19], where NMR and μ SR studies suggested the SMAF to be parasitic [20,21]. Accordingly, to identify the HO in URu_2Si_2 it is essential to resolve the nature of the SMAF and the symmetry relationship of HO and LMAF.

It was long suspected that the conflicting results are due to a distribution of lattice distortions arising from defects. Notably, uniaxial stress studies showed that LMAF is stabilized if the c/a ratio η of the tetragonal crystal is increased by the small amount $\Delta\eta_c/\eta \approx 5 \times 10^{-4}$ [22]. Hence, the SMAF may in principle result from a distribution of η across the sample, with its magnitude depending on sample quality and experimental conditions. In particular, differences of compressibility of wires, sample supports, or strain gauges that are welded, glued, or soldered to the samples will forcibly generate uncontrolled local strains that strongly affect any conclusions about the SMAF signal (see, e.g., Refs. [15–18]).

In this Letter we report for the first time *simultaneous* microscopic measurements of the lattice constants, the distribution of the lattice constants, and the antiferromagnetic moment of URu_2Si_2 as a function of temperature for pressures up to 18 kbar. To obtain these data we used for the first time a novel neutron scattering technique called Larmor diffraction (LD) to establish parasitic phases, additionally combining it with conventional diffraction. This allows us to study samples that are completely free to float in the pressure transmitting medium, thereby experiencing essentially ideal hydrostatic pressure conditions. Our data of the distribution of lattices constants $f(\Delta\eta/\eta)$ establishes *quantitatively* that the SMAF must be purely parasitic. In addition, we find a rather abrupt transition from

HO to LMAF which extends from $T = 0$ up to a bicritical point (preliminary data of $T_N(p)$ were reported in [23]). Our study demonstrates that the transition from HO to LMAF is intrinsically first order; i.e., the HO and LMAF *must* have different symmetry.

Larmor diffraction permits high-intensity measurements of lattice constants with an unprecedented high resolution of $\Delta a/a \approx 10^{-6}$ [24,25]. As shown in Fig. 1(a) in LD the sample is illuminated by a polarized neutron beam (arrows indicate the polarization). The radio frequency spin flipper coils, denoted as C1 through C4, continuously change the polarization direction of the beam as a function of time. Coils C1 and C3 are set up such that they generate a time dependence of the polarization as if the polarization would precess in the scattering plane at twice the radio frequency ω of the coils. Coils C2 and C4 are then tuned to terminate this time dependence of the polarization; at any given location in the gray shaded regime the beam polarization hence appears to precess even though there is no applied magnetic field. Coils C1 through C4 are aligned *parallel* to the lattice planes, because this way changes of the lattice spacing a sensitively affect the total time of travel t_{tot} along $L = L_1 + L_2$ (t_{tot} is purely determined by the velocity component v_p of the neutrons parallel to \vec{G}). The total phase of precession Φ along L_1 plus L_2 depends linearly on the lattice constant a : $\Phi = 2\omega L m a / (\pi \hbar)$ (m is the mass of the neutron [24–26]). Changes of a affect hence the angle α and thus the intensity recorded by the polarization analyzer and detector AD.

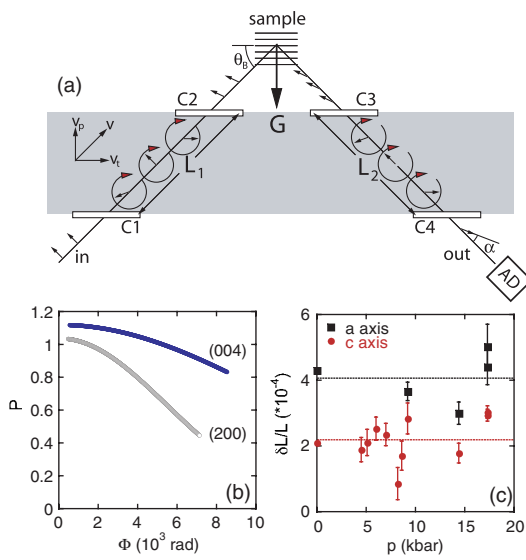


FIG. 1 (color online). (a) Schematic of Larmor diffraction [24,25]; C1 through C4 are radio frequency spin flipper coils, \vec{G} is the reciprocal lattice vector; Θ_B is the Bragg angle; AD is the polarization analyzer and detector. See text for details. (b) Typical variation of the polarization P as a function of the total Larmor phase Φ . (c) Pressure dependence of the distribution of lattice-constants for the a and c axis. With increasing pressure the width is essentially unchanged.

Our LD measurements were carried out at the spectrometer TRISP at FRM II (Munich). The temperature and pressure dependence of the lattice constants was inferred from the (400) Bragg peak for the a axis and the (008) Bragg peak for the c axis, where high resolution data at (200) and (004) could only be taken at $p = 0$ due to the absorption by the pressure cell. The magnetic ordered moment was monitored with the same setup using conventional diffraction. For our studies a Cu:Be clamp cell was used with a Fluorinert mixture [27]. The pressure was inferred at low temperatures from the (002) reflection of graphite as well as absolute changes of the lattice constants of URu_2Si_2 taking into account published values of the compressibility. The potential of LD in high-pressure studies was first demonstrated in Ref. [26].

The single crystal studied was grown by means of an optical floating-zone technique at the Amsterdam/Leiden Center. High sample quality was confirmed via x-ray diffraction and detailed electron probe microanalysis. Samples cut off from the ingot showed good resistance ratios (20 for the c axis and ≈ 10 for the a axis) and a high superconducting transition temperature $T_c \approx 1.5$ K. The magnetization of the large single crystal agreed very well with data shown in Ref. [28] and confirmed the absence of ferromagnetic inclusions. Most importantly, in our neutron scattering measurements we found an antiferromagnetic moment $m_s \approx 0.012 \mu_B$ per U atom, which matches the smallest moment reported so far [19].

As the Larmor phase Φ is proportional to the lattice constant a , the dependence of the polarization P on Φ reflects the distribution of lattice constants across the entire sample volume [25]. We have therefore measured $P(\Phi)$ over a wide range to establish if the distribution of the c/a ratios of the lattice constants may be responsible for AF order in parts of the sample. Note that this aspect of Larmor diffraction has so far only been exploited in proof of principle studies in Al alloys [24].

As shown in Fig. 1(b) $P(\Phi)$ at $p = 0$ decreases as a function of Φ , where depolarizing effects by the instrument were corrected by means of a calibration with a high quality Ge single crystal. Note that the wavelength dependence of the polarizer causes a well-understood overcorrection by a constant value [$P > 1$ in Fig. 1(b)], that leaves the measured decrease of P with Φ and hence the value of η unchanged. Assuming a Gaussian distribution of both lattice constants, we find a full width at half-maximum of $f(\Delta \eta / \eta)_{\text{FWHM}} \approx 6.4 \times 10^{-4}$. Recalling that the tail of the Gaussian distribution beyond $\Delta \eta_c / \eta \approx 5 \times 10^{-4}$ represents the sample's volume fraction in which LMAF forms [22], an average magnetic moment of $0.013(5) \mu_B$ is expected in our sample. This is in excellent quantitative agreement with the experimental value and identifies the SMAF as being purely parasitic.

As a function of pressure the distribution of lattice constants, remains essentially unchanged [Fig. 1(c)]. Thus the HO to LMAF transition is not accompanied by changes of the distribution of lattice constants. In addition

the size of m_s , which remained unchanged tiny after releasing the pressure in different sections of the single crystal underscores excellent pressure conditions.

We turn to the temperature dependence of the lattice constants and its change with pressure. At $p = 0$ in a wide temperature range below room temperature (not shown) the thermal expansion is positive for both axes [29]. However, for the c axis, the lattice constant shows a minimum close to 40 K and turns negative at lower temperatures. This general behavior is unchanged under pressure. Shown in Fig. 2 are typical low-temperature data for the a and c axis. At ambient pressure T_0 can be barely resolved. However, when crossing $p_c \approx 4.5$ kbar a pronounced additional signature emerges rapidly and merges with T_0 . Measurements of the antiferromagnetic moment (see below), identify this anomaly as the onset of the LMAF order below its T_N . At the transition the lattice constants for the a and c axes show a pronounced contraction and expansion, respectively.

The pressure and temperature dependence of m_s determined at (100) is shown in Fig. 3(a). Close to $p_c \approx 4.5$ kbar, where T_N is near base temperature, we observe first evidence of the LMAF magnetic signal, which rises steeply and already reaches almost its high-pressure limit at 5 kbar Fig. 3(b). The pressure dependence was determined by assuming the widely reported high-pressure

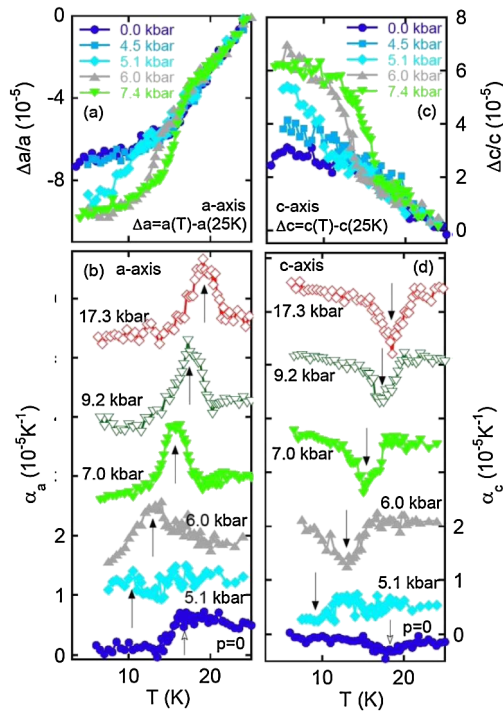


FIG. 2 (color online). Temperature dependence of the lattice constants and thermal expansion at various pressures. The HO and LMAF transitions are indicated by empty and filled arrows, respectively. (a) Data for the a axis; (b) thermal expansion of the a axis derived from the data in (a). (c) Data for the c axis; (d) thermal expansion of the c axis derived from the data in (c).

value of $m_s = 0.4\mu_B$ and comparing the magnetic (100) and nuclear (004) peak intensity.

The temperature-pressure phase diagram shown in Fig. 3(c) displays T_0 and T_N taken from the magnetic Bragg peak [Fig. 3(a)] and from the Larmor diffraction data (Fig. 2), respectively. The different data sets show excellent agreement. The main results shown in Fig. 3 are (i) the very small value of $0.012\mu_B$ of the average low-temperature ordered moment at zero pressure, (ii) a particularly abrupt increase of the low-temperature moment at $p_c \approx 4.5$ kbar (as compared to previous studies [15–19]), (iii) the steep slope of the HO–LMAF phase boundary, and (iv) the merging of the HO–LMAF phase boundary with the T_0 transition lines at approximately 9 kbar. Figure 2(b) shows that we can follow this phase boundary from low T up to T_0 .

Most importantly, (iv) implies that HO and LMAF are intrinsically separated by a phase boundary which has to be of first order with a bicritical point at 9 kbar and 18 K, since three second-order phase transition lines cannot meet in one point. (The phase boundaries from the HO and LMAF to the disordered high-temperature phase are already known to be of second order from qualitative heat capacity measurements [1,17].) This conclusion is perfectly consistent with (ii) and (iii) and excludes a linear coupling between the HO and LMAF [9].

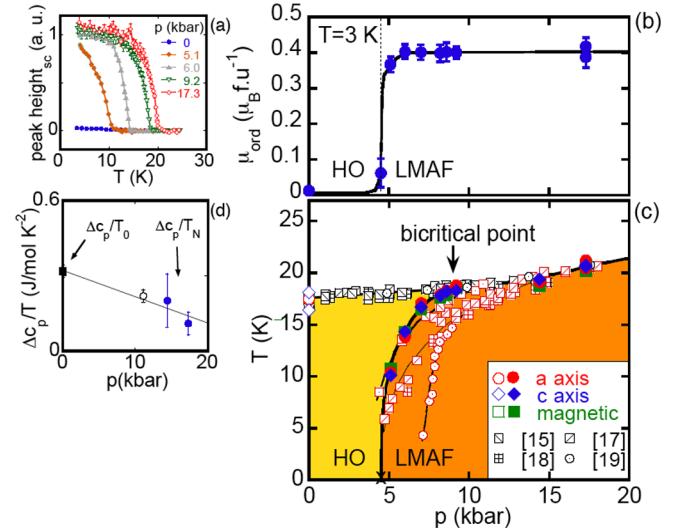


FIG. 3 (color online). Key features and pressure versus temperature phase diagram of URu_2Si_2 . (a) Temperature dependence of the magnetic peak height at various pressures. (b) Pressure dependence of the low-temperature magnetic moment m_s . (c) Phase diagram based on Larmor diffraction and conventional magnetic diffraction data. The onset of LMAF and HO in our data is marked by full and empty symbols, respectively (x marks a transition near base temperature). For better comparison data of T_N and T_0 from Refs. [15,17–19] are shown, where symbols with bright contours refer to T_N and symbols with dark contours to T_0 . (d) Specific-heat jump derived from thermal-expansion data via the Ehrenfest relation (full circles). Heat capacity data is taken from Refs. [1] (square) and [17] (empty circle).

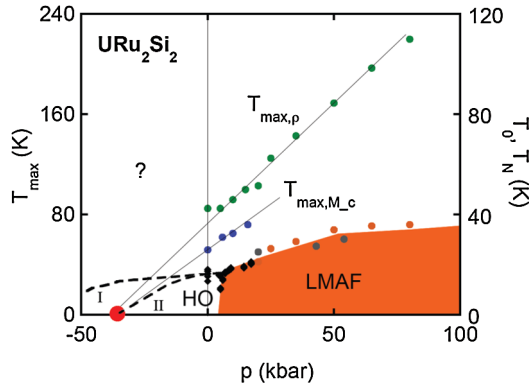


FIG. 4 (color online). Extended phase diagram of URu_2Si_2 based on the data presented here (diamonds) and signatures in resistivity (bright [34] and dark [17] circles along the PM-LMAF boundary). $T_{\max,\rho}$ and T_{\max,M_c} denote coherence maxima in the resistivity [34] and magnetization [28], respectively. The HO might either mask a QCP (I) or replace LMAF (II) near quantum criticality.

Although our results show that the HO and LMAF must have different symmetry, they also suggest that both types of order may have a common origin. Using the Ehrenfest relation, we have converted our thermal-expansion data into a background-free estimate of the specific-heat jump, ΔC , at the PM to LMAF transition. Figure 3(d) shows a continuous evolution with pressure of the specific-heat jumps at the LMAF to PM and corresponding HO to PM transitions. The common origin of both phases may in fact be related to results of recent inelastic neutron scattering studies as discussed in the context of recent band structure calculations [30]. Notably, excitations at $(1,0,0)$ appear only in the HO phase and may be its salient characteristic [31]. However, excitations at $(1.4,0,0)$ in the PM state become gapped in both the HO and LMAF state and have been quantitatively linked to the specific-heat jump at $p = 0$ [32].

Our study finally allows us to speculate on a new route to the HO illustrated in Fig. 4, which summarizes the pressure dependence of features in the resistivity and magnetization, usually denoted as Kondo or coherence temperature T_{coh} . Remarkably, these features all seem to extrapolate to the same negative critical pressure, suggesting the possible existence of an AF quantum critical point (QCP). Thus the HO in URu_2Si_2 may emerge from quantum criticality, possibly even masking an AF QCP (case I in Fig. 4). Alternatively, both HO and LMAF might only exist below T_{coh} (case II), with pressure tipping the balance between the two. The latter has been suggested in a recent proposal, where HO and LMAF are believed to be different variants of the same underlying complex order parameter [33]. The pressure dependence of ΔC thereby sets constraints on any theory of the HO involving quantum criticality.

In conclusion, we demonstrate quantitatively that the SMAF in URu_2Si_2 is purely parasitic. The excellent experimental conditions allow us to resolve that the HO and LMAF are intrinsically separated by a line of first-order

transitions ending in a bicritical point. Hence the HO and LMAF cannot have the same symmetry. This supports exotic scenarios of the HO such as incommensurate orbital currents, helicity order, or multipolar order.

We are grateful to P. Böni, A. Rosch, A. de Visser, K. Buchner, F. M. Grosche, and G. G. Lonzarich for support and stimulating discussions. We thank FRM II for general support. C. P. and M. V. acknowledge support through DFG FOR 960 (quantum phase transitions) and M. V. also acknowledges support through DFG SFB 608.

- [1] T. T. M. Palstra *et al.*, Phys. Rev. Lett. **55**, 2727 (1985).
- [2] M. B. Maple *et al.*, Phys. Rev. Lett. **56**, 185 (1986).
- [3] W. Schlabitz *et al.*, Z. Phys. B **62**, 171 (1986).
- [4] C. Broholm *et al.*, Phys. Rev. Lett. **58**, 1467 (1987).
- [5] H. Amitsuka *et al.*, Phys. Rev. Lett. **83**, 5114 (1999).
- [6] L. P. Gor'kov and A. Sokol, Phys. Rev. Lett. **69**, 2586 (1992).
- [7] D. F. Agterberg and M. B. Walker, Phys. Rev. B **50**, 563 (1994).
- [8] N. Shah *et al.*, Phys. Rev. B **61**, 564 (2000).
- [9] V. P. Mineev and M. E. Zhitomirsky, Phys. Rev. B **72**, 014432 (2005).
- [10] P. Chandra *et al.*, Nature (London) **417**, 831 (2002).
- [11] A. Kiss and P. Fazekas, Phys. Rev. B **71**, 054415 (2005).
- [12] C. M. Varma and L. Zhu, Phys. Rev. Lett. **96**, 036405 (2006).
- [13] F. Bourdarot *et al.*, Physica (Amsterdam) **359B–361B**, 986 (2005).
- [14] J. R. Jeffries *et al.*, J. Phys. Condens. Matter **20**, 095225 (2008).
- [15] G. Motoyama, T. Nishioka, and N. K. Sato, Phys. Rev. Lett. **90**, 166402 (2003).
- [16] S. Uemura *et al.*, J. Phys. Soc. Jpn. **74**, 2667 (2005).
- [17] E. Hassinger *et al.*, Phys. Rev. B **77**, 115117 (2008).
- [18] G. Motoyama *et al.*, J. Phys. Soc. Jpn. **77**, 123710 (2008).
- [19] H. Amitsuka *et al.*, J. Magn. Magn. Mater. **310**, 214 (2007).
- [20] K. Matsuda *et al.*, J. Phys. Condens. Matter **15**, 2363 (2003).
- [21] A. Amato *et al.*, J. Phys. Condens. Matter **16**, S4403 (2004).
- [22] M. Yokoyama *et al.*, Phys. Rev. B **72**, 214419 (2005).
- [23] P. G. Niklowitz *et al.*, Physica (Amsterdam) **404B**, 2955 (2009).
- [24] M. T. Rekveldt *et al.*, Europhys. Lett. **54**, 342 (2001).
- [25] T. Keller *et al.*, Appl. Phys. A Suppl. **74**, s332 (2002).
- [26] C. Pfleiderer *et al.*, Science **316**, 1871 (2007).
- [27] C. Pfleiderer *et al.*, J. Phys. Condens. Matter **17**, S3111 (2005).
- [28] C. Pfleiderer, J. A. Mydosh, and M. Vojta, Phys. Rev. B **74**, 104412 (2006).
- [29] A. de Visser *et al.*, Phys. Rev. B **34**, 8168 (1986).
- [30] S. Elgazzar *et al.*, Nature Mater. **8**, 337 (2009).
- [31] A. Villaume *et al.*, Phys. Rev. B **78**, 012504 (2008).
- [32] C. R. Wiebe *et al.*, Nature Phys. **3**, 96 (2007).
- [33] K. Haule and G. Kotliar, arXiv:0907.3889; arXiv:0907.3892.
- [34] T. Kagayama *et al.*, J. Alloys Compd. **213–214**, 387 (1994).